

# UC Davis

## UC Davis Previously Published Works

### Title

Identification and characterization of a natural polymorphism in FT-A2 associated with increased number of grains per spike in wheat

### Permalink

<https://escholarship.org/uc/item/7sx8s0k1>

### Journal

Theoretical and Applied Genetics, 135(2)

### ISSN

0040-5752

### Authors

Glenn, Priscilla  
Zhang, Junli  
Brown-Guedira, Gina  
[et al.](#)

### Publication Date

2022-02-01

### DOI

10.1007/s00122-021-03992-y

Peer reviewed

1     **Identification and characterization of a natural polymorphism in *FT-A2* associated with**  
2                                   **increased number of grains per spike in wheat**

3  
4     Priscilla Glenn<sup>1</sup>, Junli Zhang<sup>1</sup>, Gina Brown-Guedira<sup>2</sup>, Noah DeWitt<sup>3</sup>, Jason P. Cook<sup>4</sup>, Kun Li<sup>1,5</sup>,  
5                                   Eduard Akhunov<sup>6</sup>, Jorge Dubcovsky<sup>1,5</sup>

6  
7     <sup>1</sup> Department of Plant Sciences, University of California, Davis, CA 95616, USA.

8     <sup>2</sup> USDA-ARS Plant Science Research, Raleigh, NC 27695, USA.

9     <sup>3</sup> Department of Crop and Soil Sciences, North Carolina State University, Raleigh, NC 27695, USA.

10    <sup>4</sup> Department of Plant Sciences and Plant Pathology, Montana State Univ., Bozeman, MT, USA

11    <sup>5</sup> Howard Hughes Medical Institute, Chevy Chase, MD 20815, USA.

12    <sup>6</sup> Department of Plant Pathology, Kansas State University, Manhattan, KS 66506, USA.

13

14    Priscilla Glenn: ORCID 0000-0002-2200-7241

15    Junli Zhang: ORCID 0000-0001-6625-2073

16    Gina Brown-Guedira: ORCID 0000-0002-1958-2827

17    Noah DeWitt: ORCID 0000-0001-9055-993X

18    Jason Cook: ORCID 0000-0002-7753-6191

19    Kun Li: ORCID 0000-0001-8308-1560

20    Eduard Akhunov: ORCID 0000-0002-0416-5211

21    Jorge Dubcovsky: ORCID 0000-0002-7571-4345

22

23    **# Corresponding author**

24    Jorge Dubcovsky. E-mail: [jdubcovsky@ucdavis.edu](mailto:jdubcovsky@ucdavis.edu), Phone: +1-530-902-8178.

25                                   ORCID: 0000-0002-7571-4345.

26

27    **Short Title:** *FT-A2* polymorphism increases grain number per spike

28

29    **Key words:** wheat, yield components, spikelet number, grain number, fertility

30

31 **Abstract**

32 Increases in wheat grain yield are necessary to meet future global food demands. A previous  
33 study showed that loss-of-function mutations in *FLOWERING LOCUS T2 (FT2)* increase  
34 spikelet number per spike (SNS), an important grain yield component. However, these mutations  
35 were also associated with reduced fertility, offsetting the beneficial effect of the increases in SNS  
36 on grain number. Here, we report a natural mutation resulting in an aspartic acid to alanine  
37 change at position 10 (D10A) associated with significant increases in SNS and no negative  
38 effects on fertility. Using a high-density genetic map, we delimited the SNS candidate region to a  
39 5.2 Mb region on chromosome 3AS including 28 genes. Among them, only *FT-A2* showed a  
40 non-synonymous polymorphism (D10A) present in two different populations segregating for the  
41 SNS QTL on chromosome arm 3AS. These results, together with the known effect of the *ft-A2*  
42 mutations on SNS, suggest that variation in *FT-A2* is the most likely cause of the observed  
43 differences in SNS. We validated the positive effects of the A10 allele on SNS, grain number,  
44 and grain yield per spike in near-isogenic tetraploid wheat lines and in an hexaploid winter wheat  
45 population. The A10 allele is present at very low frequency in durum wheat and at much higher  
46 frequency in hexaploid wheat, particularly in winter and fall-planted spring varieties. These  
47 results suggest that the *FT-A2* A10 allele may be particularly useful for improving grain yield in  
48 durum wheat and fall-planted common wheat varieties.

49

50 **Key message**

51 We discovered a natural *FT-A2* allele that increases grain number per spike in both pasta and  
52 bread wheat with limited effect on heading time.

53

## 54 **Introduction**

55 Wheat is a global crop of major economic value and nutritional importance as it provides around  
56 20% of the calories and protein consumed by the human population  
57 (<http://www.fao.org/faostat/en/#data/FBS>). However, with ever changing environmental  
58 conditions and the rising human population, it is critical to increase wheat grain yield to meet  
59 future demands. Yield is a multifaceted trait that can be partitioned into several yield  
60 components, including spikes per unit of area, spikelet number per spike (SNS), grains per  
61 spikelet, and grain weight. Several genes have been identified that affect these grain yield  
62 components (Kuzay et al. 2019; Li et al. 2019; Poursarebani et al. 2015; Sakuma et al. 2019;  
63 Shaw et al. 2013; Simmonds et al. 2016; Wang et al. 2019).

64 Many of the genes affecting SNS also have strong effects on flowering time that can limit their  
65 use in variety development. Flowering before or after the optimum flowering time can result in  
66 yield penalties due to reduced fertility or increased risks of frost or heat damage, respectively.

67 The vernalization gene *VRN1* is a good example of a gene affecting both flowering time and  
68 SNS. The *vrn1*-null mutant significantly increases SNS by delaying the transition of the  
69 inflorescence meristem to a terminal spikelet, but also delays the transition of the vegetative  
70 meristem to inflorescence meristem, resulting in a very late heading time (Li et al. 2019).

71 Another good example is the main wheat photoperiod gene *PHOTOPERIOD1* (*PPD1*), which  
72 shows a strong correlation between heading date and SNS in lines carrying different dosages of  
73 *PPD1* loss-of-function mutations ( $R^2= 0.74$ ) (Shaw et al. 2013). A correlation between heading  
74 date and SNS has also been observed in genes regulated by *PPD1* such as the *FLOWERING*  
75 *LOCUS T1* gene (*FT1*) (Brassac et al. 2021; Finnegan et al. 2018; Isham et al. 2021; Lv et al.  
76 2014).

77 *FT1* encodes a mobile protein that travels through the phloem and carries environmental signals  
78 from the leaves to the shoot apical meristem (SAM), where it forms a complex with 14-3-3 and  
79 FD-like proteins (Florigen Activation Complex) (Taoka et al. 2011). This complex binds to the  
80 promoter of the meristem identity gene *VERNALIZATION1* (*VRN1*), promoting its expression  
81 and the transition from the vegetative to the reproductive phase in wheat (Li et al. 2015).

82 Induction of *FT1* also results in the upregulation of *SUPPRESSOR OF OVEREXPRESSION OF*  
83 *CONSTANS1-1* (*SOC1*), *LEAFY* (*LFY*) and genes in the gibberellin (GA) pathway that are

84 essential for spike development and stem elongation (Pearce et al. 2013). A deletion of *FT-B1* in  
85 hexaploid wheat delays the transition to reproductive growth and increases SNS (Finnegan et al.  
86 2018).

87 In addition to *FT1*, wheat has at least five *FT-like* paralogs designated as *FT2* to *FT6* (Lv et al.  
88 2014), which have some overlapping functions but also varying degrees of sub-functionalization  
89 (Halliwell et al. 2016; Lv et al. 2014). *FT2* is the most similar paralog to *FT1* (78% protein  
90 identity), but the two genes still exhibit marked differences in transcription and protein  
91 interaction profiles. Whereas the FT1 protein interacts with five out of the six wheat 14-3-3  
92 proteins tested so far, FT2 failed to interact with any of these members of the Florigen Activation  
93 Complex (Li et al. 2015). The two genes also differ in their temporal and spatial transcription  
94 profiles. *FT1* transcript levels in the leaves are upregulated earlier than *FT2* when plants are  
95 grown at room temperature, but only *FT2* is induced when plants are grown for a long period at 4  
96 °C (vernalization) (Shaw et al. 2019). Interestingly, *FT2* is the only member of the wheat *FT-like*  
97 gene family that is expressed directly in the shoot apical meristem (SAM) and in the developing  
98 spike (Lv et al. 2014), in addition to leaves and elongating stems (Fig. S1).

99 Loss-of-function mutations in *FT2*, identified in a sequenced mutant population of the tetraploid  
100 wheat variety Kronos (Krasileva et al. 2017), resulted in limited differences in heading time but  
101 significantly increased SNS (Shaw et al. 2019). Similar increases in SNS were observed in *ft-B2*  
102 natural mutants detected in hexaploid wheat (Gauley et al. 2021). The loss-of function mutation  
103 in the A-genome copy of *FT2* (*FT-A2*) in Kronos was associated with significantly larger  
104 increases in SNS (10-15%) than the mutation in the B-genome copy (*FT-B2*, 2-5%). This  
105 difference in SNS was associated with much higher transcript levels of *FT-A2* relative to *FT-B2*  
106 in all tissues and developmental stages (Fig. S1). The increases in spikelet number in the double  
107 *ft-A2 ft-B2* mutant (henceforth *ft2*-null) were significantly larger than in the single *ft-A2* mutant  
108 confirming that the *FT-B2* gene still has a residual effect on SNS in spite of its lower transcript  
109 levels.

110 The increase in SNS in the *ft-A2* mutant was associated with reduced fertility, offsetting the  
111 potential positive effects of the increase in SNS on total grain yield (Shaw et al. 2019). This  
112 effect was observed in growth chambers under optimal conditions suggesting that is not an  
113 indirect effect of altered flowering time. We hypothesized that strong selection in cultivated

114 wheat for grain yield might have selected an *FT-A2* variant with a positive effect on SNS, but  
115 without the associated negative effect on fertility. Analysis of natural variation in *FT-A2* revealed  
116 an aspartic acid to alanine change at position 10 (D10A) that was rare in tetraploid wheat but  
117 frequent in modern common wheat varieties, suggesting positive selection for the new allele. In  
118 this study, we characterized the effect of the D10A polymorphism on wheat heading time, SNS,  
119 grain number, and spike yield in different wheat classes and performed a high-density genetic  
120 mapping of the SNS QTL that identified *FT-A2* as the most likely candidate gene.

121

## 122 **Material and Methods**

123 Analysis of the exome capture data generated by the WheatCAP project using the assay  
124 developed by NimbleGen (Krasileva et al. 2017) and deposited in the Wheat T3 database  
125 (<https://wheat.triticeaetoolbox.org/>) revealed the existence of an A to C SNP within the *FT-A2*  
126 coding region that resulted in the D10A polymorphism. We studied the effect of this SNP on  
127 heading time, SNS, grain number, and spike yield in two segregating populations in tetraploid  
128 and hexaploid wheat.

### 129 **Biparental mapping population in tetraploid wheat (*Triticum turgidum* ssp. *durum*)**

130 The tetraploid mapping population included 163 BC<sub>1</sub>F<sub>2</sub> lines from the cross Kronos \*2/Gredho  
131 (designated KxG hereafter). Kronos (PI 576168, *FT-A2* D10 allele) is a semi-dwarf (*Rht-B1b*),  
132 with reduced photoperiod sensitivity (*Ppd-A1a*) spring wheat, whereas Gredho (PI 532239, *FT-*  
133 *A2* A10 allele) is a tall (*Rht-B1a*), photoperiod sensitive (*Ppd-A1b*) spring landrace from Oman.  
134 We planted the KxG population as headrows in 2015-2016 season at the UC Experimental Field  
135 Station in Davis, CA with each row including on average five individual plants.

### 136 **Near isogenic lines of the *FT-A2* A10 allele from Gredho into Kronos**

137 We also evaluated the effect of the *FT-A2* alleles in two sets of near isogenic lines (NILs). For  
138 the first set, we selected *FT-A2* heterozygous BC<sub>1</sub>F<sub>2</sub> and BC<sub>1</sub>F<sub>3</sub> lines from the cross Kronos  
139 \*2/Gredho and selected two sets of homozygous BC<sub>1</sub>F<sub>3-4</sub> homozygous A10 and D10 sister lines  
140 using the *FT-A2* marker (H2-14 and H2-23). These lines were semi-dwarf and carried the *Ppd-*  
141 *A1a* allele for reduced photoperiod sensitivity and the *Vrn-A1* allele for spring growth habit. We  
142 used the BC<sub>1</sub>F<sub>3-5</sub> grains produced by these plants for two field experiments, one at the University

143 of California, Davis (UCD) and the other one at Tulelake (California northern intermountain  
144 region). Both field experiments were organized in a complete randomized design with plants as  
145 experimental units. Three to five spikes were measured per plant and averaged for 10 plants per  
146 genotype at the UC Davis experiment. In the Tulelake experiment, 23-27 spikes per genotype  
147 were randomly collected and used as experimental units in the statistical analyses.

148 In parallel, we backcrossed the A10 allele into Kronos for three additional generations (Kronos  
149 \*5/Gredho), and then selected BC<sub>4</sub>F<sub>2</sub> NILs homozygous for the A10 and D10 alleles using the  
150 *FT-A2* molecular marker. The BC<sub>4</sub>F<sub>3</sub> seed was increased in the greenhouse in 2020 and the  
151 BC<sub>4</sub>F<sub>4</sub> grains were used for field experiments at UCD and Tulelake in 2021 that used small plots  
152 (four 1-m rows, 1.1 m<sup>2</sup>) as experimental units, organized in a randomized complete block design  
153 with 12 blocks. Grains of the BC<sub>4</sub>F<sub>4</sub> Kronos isogenic line with the A10 allele were deposited in  
154 the National Small Grain Collection as PI 699107.

### 155 **Biparental mapping population in hexaploid winter wheat**

156 The hexaploid population included 358 F<sub>5</sub>-derived recombinant inbred lines (RILs) derived from  
157 the cross between soft-red winter wheat lines LA95135 (CL-850643/PIONEER-  
158 2548//COKER9877/3/FL-302/COKER-762) x SS-MVP57 (FFR555W/3/VA89-22-  
159 52/TYLER//REDCOAT\*2/GAINES). LA95135 is semidwarf (*Rht-D1b*) and photoperiod  
160 sensitive (*Ppd-D1b*), whereas SS-MVP57 is tall (*Rht-D1a*) and has reduced photoperiod  
161 sensitivity (*Ppd-D1a*) (DeWitt et al. 2021). This winter wheat population was previously  
162 genotyped and phenotyped as 1 m rows in the field at Raleigh, NC and Kinston, NC during the  
163 2017-2018 season, and in Raleigh, Kinston, and Plains, GA in the 2018-2019 season (DeWitt et  
164 al. 2021). These locations will be referred to as Raleigh (Ral), Kinston (Kin), and Plains (Pla)  
165 followed by the harvest year (18 or 19).

### 166 ***FT-A2* marker development and allelic frequencies**

167 We targeted the *FT-A2*, D10A SNP at position 124,172,909 bp (RefSeq v1.0) on chromosome  
168 3A with a Cleaved Amplified Polymorphic Sequence (CAPS) marker. Primers FT-A2-D10A  
169 forward and reverse (Table S1) amplify a fragment of 705 bp. After digestion with the restriction  
170 enzyme *ApaI*, the fragment amplified from the D10 allele remained undigested, whereas the  
171 fragment amplified from the A10 allele was digested into two fragments of 448 and 257 bp.

172 We used this marker to determine the frequency of the D10A mutation in 89 *T. urartu*, 82 *T.*  
173 *turgidum* ssp. *dicoccoides*, 32 *T. turgidum* ssp. *dicoccon*, 417 *T. turgidum* ssp. *durum* and 705 *T.*  
174 *aestivum* accessions summarized in Supplementary Appendix S1. Among the hexaploid lines, we  
175 included a collection of 238 landraces and varieties (He et al. 2019) and a set of 126 winter  
176 wheats (T3/Wheat) genotyped by exome capture and with data for the *FT-A2* D10A  
177 polymorphism. We also used the *FT-A2* marker to genotype a panel of 242 spring wheats with  
178 reduced photoperiod sensitivity (Zhang et al. 2018) and a panel of 99 varieties and modern  
179 breeding lines from the Montana State University wheat breeding program (Supplementary  
180 Appendix S1). Based on the planting season used in the area where the spring varieties were  
181 developed, they were divided into those developed under spring planting (hereafter "DuS") or  
182 under fall planting (hereafter "DuF"). A previous study has previously shown that DuS and DuF  
183 groups are genetically differentiated using the 90K SNP array (Zhang et al. 2018)  
184 (Supplementary Appendix S1).

### 185 **High resolution genetic map**

186 The high-resolution map of the KxG population was developed in two phases. In the first phase,  
187 we identified two BC<sub>1</sub>F<sub>3</sub> plants from the KxG BC<sub>1</sub>F<sub>2</sub> head rows, H2 and D12, which were  
188 heterozygous for *FT-A2* candidate region. From these heterozygous lines we generated large  
189 segregating Heterogeneous Inbred Families (HIF) populations to identify recombination events  
190 within the *FT-A2* candidate region. For phenotypic screenings, these recombinants were space-  
191 planted at least three inches apart in a completely randomized design. Additional markers in the  
192 candidate gene region were developed for 11 genes on both sides of *FT-A2* covering a region of  
193 ~10 Mb using the exome capture sequence data from Kronos and Gredho (Table S1).

### 194 **Statistical analysis**

195 In the tetraploid biparental population, we analyzed the effect of the *FT-A2* alleles with a 3 x 2  
196 factorial ANOVA that included the genotypic variation at *PPD-A1* and *RHT-B1* as additional  
197 factors, since both genes are known to have pleiotropic effects on heading time and yield  
198 components. In the hexaploid winter wheat population, we analyzed the effect of the *FT-A2* in a  
199 4 x 2 factorial ANOVA including the segregating genes *PPD-D1*, *RHT-D1* and *WHEAT*  
200 *ORTHOLOG OF APO1 (WAPO-A1)*, which was previously shown to affect SNS (Kuzay et al.



201 2019). Analysis of Variance was conducted with the “Anova” function in R package “car” (Fox  
202 et al. 2019) with type 3 sum of squares.

### 203 **Yeast two-hybrid assays**

204 Modified Gateway (Invitrogen) bait/prey vectors pLAW10 and pLAW11 (Cantu et al. 2013) and  
205 yeast strain Y2HGold (Clontech, Mountain View, CA, USA) were used in the yeast two-hybrid  
206 assays. pLAW10 is the Gateway version of pGBKT7 (GAL4 DNA-binding domain, BD) and  
207 pLAW11 is the Gateway version of pGADT7 (GAL4 activation domain, AD). For all Gateway  
208 compatible cloning, pDONR/Zeo (Life Technologies, Grand Island, NY, USA) was used to  
209 generate the entry vectors. All constructs were verified by sequencing. Yeast two-hybrid assays  
210 were performed according to the manufacturer’s instructions (Clontech). Transformants were  
211 selected on SD medium lacking leucine (-L) and tryptophan (-W) plates and re-plated on  
212 SD medium lacking -L, -W, histidine (-H) and adenine (-A) to test the interactions.

213

## 214 **Results**

### 215 **Natural variation in *FT-A2***

216 We used exome capture data deposited in the T3 database (<https://triticeaetoolbox.org/wheat/>) to  
217 explore the natural polymorphisms in *FT-A2*. We identified an A to C SNP at position  
218 124,172,909 in chromosome arm 3AS of the Chinese Spring (CS) RefSeq v1.0, which resulted in  
219 an amino acid change at position 10 of the FT-A2 protein from aspartic acid (D) to alanine (A)  
220 (henceforth, D10 and A10 alleles). In the analyzed accessions of *T. urartu*, *T. turgidum* ssp.  
221 *dicoccoides* and *T. turgidum* ssp. *dicoccon*, we detected only the D10 allele (Table 1). D10 was  
222 also the only allele detected in all the other grass species we analyzed including *Lolium perenne*  
223 (AMB21802), *Oryza sativa* (XP\_021310907), *Zea mays* (NP\_001106251), and *Panicum*  
224 *virgatum* (APP89655), indicating that D10 is the ancestral allele. In this study, we describe the  
225 change from the ancestral to the derived allele (D10A) rather than relative to the Chinese Spring  
226 (CS) reference genome that carries the derived A10 allele,

227 We also screened a collection of 417 *T. turgidum* ssp. *durum* accessions with a CAPS marker for  
228 the D10A polymorphism (see Material and Methods) and found that only 0.7% carried the A10  
229 allele (Table 1). Two of the three accessions with the A10 allele were from Oman (PI 532239 =

230 ‘Gredho’ and PI 532242, ‘Musane and Byaza’) and the other one was from Turkey (PI 167718),  
231 suggesting that the A10 allele is almost absent from modern Western durum germplasm.

232 We detected a higher frequency of the A10 allele (56.5 %) among 705 *T. aestivum* ssp. *aestivum*  
233 lines (Table 1). This overall frequency was similar to that detected in a worldwide collection of  
234 landraces and varieties combining winter and spring lines (59.7 %) (He et al. 2019). We also  
235 analyzed the frequency of the D10A polymorphisms in two collections with known growth habit,  
236 and found a higher frequency of the A10 allele among the winter lines (81.7 %) than among the  
237 spring lines (44.9 %, Table 1). Among the 341 spring wheat lines genotyped with the *FT-A2*  
238 marker, we found that varieties developed under fall-planting (DuF or long cycle) had a  
239 significantly higher frequency of the A10 allele (58.4%) than those developed under spring-  
240 planting (DuS or short cycle, 34.4%,  $\chi^2 P < 0.001$ , Table 1). A complete list of the accessions  
241 used in these calculations is available in Supplementary Appendix 1, and a summary of the  
242 frequencies is presented in Table 1.

#### 243 **Effect of the D10A polymorphism in tetraploid wheat**

244 To test the effect of the D10A polymorphism on SNS, we used the diagnostic CAPS marker to  
245 screen 163 BC<sub>1</sub>F<sub>2</sub> plants from the KxG population segregating for this polymorphism. We also  
246 genotyped this population with markers for the segregating *RHT-B1* (Guedira et al. 2010) and  
247 *PPD-A1* (Wilhelm et al. 2009) genes, which can also affect SNS. Plants were grown in the field  
248 in the 2015-2016 season in Davis, CA and were phenotyped for individual plant height (HT),  
249 days to heading (DTH), and spikelet number per spike (SNS, Table 2).

250 The three-way factorial ANOVAs including *FT-A2*, *RHT-B1*, and *PPD-A1* as factors showed  
251 significant effects for SNS, HT, and DTH and no significant interactions for any of the traits. As  
252 expected, *RHT-B1* showed the strongest effect on plant height and *PPD-A1* on heading time,  
253 although both genes affected both traits (Table 2). The strongest effect on SNS was detected for  
254 *PPD-A1*, but a significant effect was also detected for *FT-A2* (Table 2), with plants homozygous  
255 for A10 showing 6.4 % higher SNS than those homozygous for D10 allele (Table 2). The  
256 differences in SNS between the *FT-A2* alleles were larger in the late flowering plants  
257 homozygous for the photoperiod sensitive allele from Gredho (2.3 spikelets/spike) than in the  
258 early flowering plants homozygous for the Kronos allele for reduced photoperiod sensitivity (1.0  
259 spikelets per spike), but the interaction was not significant.

260 **Effect of the *FT-A2* alleles in Kronos near isogenic lines**

261 To analyze the effect of the D10A polymorphism independently of the variability generated by  
262 other major genes, we evaluated two sets of near isogenic lines in field experiments in 2020  
263 (BC<sub>1</sub>F<sub>3-5</sub> sister lines) and 2021 (BC<sub>4</sub>F<sub>2-4</sub> sister lines, see Material and Methods) at UCD and  
264 Tulelake. In the 2020 experiment at UCD, lines with the A10 allele showed large and significant  
265 increases in SNS (13.8%), grain number per spike (GNS, 31.7%), grains per spikelet (16.1%,  
266 also referred to as fertility) and grain yield per spike (33.0%) relative to the sister lines  
267 homozygous for the D10 allele (Table 3). The results from this experiment were consistent  
268 between two independent pairs of BC<sub>1</sub>F<sub>3-5</sub> sister lines (H2-14 and H2-23, Table 3). The 2020  
269 experiment in Tulelake (Northern California, spring planting) using BC<sub>1</sub>F<sub>3-5</sub> sister lines from  
270 family H2-14, also showed a significant increase in SNS (4.0%), but the increases in GNS,  
271 grains per spikelet, and grain yield per spike were not significant (Table 3).

272 For the 2021 UCD experiment using 1.1 m<sup>2</sup> small plots as experimental units (12 replications),  
273 BC<sub>4</sub>F<sub>2-4</sub> lines with the A10 allele headed on average 0.8 d later than the sister lines with the D10  
274 allele ( $P = 0.0252$ ) and showed significant increases in SNS (5.7 %,  $P = 0.0011$ ) and GNS (6.3  
275 %,  $P = 0.0168$ , Table 3). In this experiment we did not detect significant differences in grains  
276 per spikelet ( $P = 0.7919$ ). We observed a negative correlation between average GNS and grain  
277 weight across the 24 plots ( $R = -0.61$ ) and a significant negative effect of the A10 allele on  
278 kernel weight (-7.8 %,  $P = 0.0002$ ). The negative effect on grain weight offset the positive effect  
279 of the A10 allele on grain number resulting in non-significant differences in grain weight per  
280 spike or per plot (Table 3).

281 For the 2021 Tulelake experiment using 1.1 m<sup>2</sup> small plots (12 replications), we included the  
282 Kronos lines with truncation mutations in *FT-A2* and *FT-B2* (*ft2*-null, henceforth) developed  
283 before (Shaw et al. 2019) in addition to the BC<sub>4</sub>F<sub>2-4</sub> Kronos lines with the D10 and A10 alleles.  
284 The lines with the A10 allele showed highly significant increases in SNS (4.1 %), GNS (6.1 %),  
285 and grain yield per spike (7.7 %), that were of similar magnitude to the ones observed in the  
286 2020 Tulelake experiment (Table 3). The null line also showed a significant increase in SNS  
287 (7.5%) relative to the wildtype Kronos (D10), but the negative impact of the *FT2* loss-of-  
288 function mutations in grains per spikelet (-9.4%) and grain weight (-7.3%) resulted in a

289 significant reduction in grain yield per spike (-9.3%, Table 3). No significant differences in grain  
290 yield per plot were detected among the three lines.

### 291 **The A10 allele has a positive effect on SNS and spike yield in winter wheat**

292 To analyze the effect of the D10A *FT-A2* alleles in winter wheat, we used phenotypic data  
293 available from 358 F<sub>5</sub>-derived RILs from the cross between soft-red winter wheat lines LA95135  
294 and SS-MVP57 (DeWitt et al. 2021) and genotypic data for the *FT-A2* marker developed in this  
295 study. This population was also segregating for *PPD-D1*, *RHT-D1*, and *WAPO-A1*, which were  
296 included as factors together with *FT-A2* in a 4 x 2 factorial ANOVA.

297 Plants carrying the *FT-A2* allele A10 (SS-MVP57) headed on average 1.7 days later ( $P < 0.001$ ,  
298 Fig. 1a) and had 0.6 more spikelet per spike (5.1 % increase,  $P < 0.001$ , Fig. 1b) than plants  
299 carrying the D10 allele (LA95135). The differences in SNS were significant in all tested  
300 locations. The A10 allele was also associated with a significant increase in GNS in the overall  
301 ANOVA ( $P < 0.001$ ), but the separate analyses of the two locations showed significant  
302 differences only at Pla19 (4.4 more grains per spike,  $P < 0.001$ , Fig. 1c). No significant effects  
303 were detected on fertility (Fig. 1d). A significant increase in spike yield was associated with the  
304 A10 allele in the overall ANOVA (average 4.6%,  $P < 0.001$ ), and two out of the three tested  
305 locations were significant in the analyses by location ( $P < 0.001$ , Fig. 1e).

### 306 **High resolution mapping of the SNS QTL on chromosome 3AS**

307 The previous results showed that the haplotypes associated with the *FT-A2* D10 and A10 alleles  
308 have a significant effect on SNS. To narrow down the candidate gene region and explore the  
309 linkage between the *FT-A2* D10A polymorphism and the differences in SNS, we generated a  
310 high-density map of the 3AS chromosome region in tetraploid wheat using a total of 3,161  
311 BC<sub>1</sub>F<sub>3</sub>, BC<sub>1</sub>F<sub>4</sub>, and BC<sub>1</sub>F<sub>5</sub> plants derived from the KxG population. These plants were screened  
312 in separate batches over three years using flanking markers 3A-117.83 and 3A-127.82 (numbers  
313 indicate coordinates in RefSeq v1.0 in Mb). Within this 9.9 Mb region including *FT-A2* (124.17  
314 Mb), we identified 76 recombination events corresponding to a genetic distance of 1.58 cM (6.26  
315 Mb per cM). One of these recombination events (H2-6-#14-5) was detected in the progeny test of  
316 primary recombinant H2-#6, which explains the presence of two close recombination events in  
317 this line (Table 4).

318 In addition to the molecular marker for the *FT-A2* D10A SNP and the two flanking markers, we  
319 developed eight more KASP and CAPS markers in the candidate region (Table S1) and used  
320 them to genotype plants carrying recombination events in the region. The lines with the 10  
321 closest recombination events to *FT-A2* are presented in Table 4 together with the results of the  
322 field progeny tests for SNS. Progenies of the lines H2-#6 and H2-14#17-2 heterozygous for *FT-*  
323 *A2* showed significant differences in SNS ( $P < 0.01$ ) between lines homozygous for the two  
324 parental alleles, whereas progeny tests for the eight lines homozygous for *FT-A2* did not show  
325 significant difference in SNS between parental alleles in the heterozygous flanking regions  
326 (Table 4). Average SNS were as expected, with the lines homozygous for the A10 allele having  
327 1.3 more spikelets on average than the lines homozygous for the D10 allele.

328 The phenotype of the critical recombinant line #18-5 with the closest distal recombination event  
329 to *FT-A2* was validated in a separate experiment in Davis in 2021 (Table S2). In this experiment,  
330 control lines showed highly significant differences in SNS ( $P < 0.0001$ ) confirming that the  
331 differences in SNS were detectable in this experiment. By contrast, there was no significant  
332 difference between the sister lines with and without the recombination event #18-5, with both  
333 lines showing SNS values similar to the control line with the Gredho allele (Table S2). Taken  
334 together, these results confirmed that the causal gene for the 3AS QTL for SNS was proximal to  
335 the marker located at CS RefSeq v1.0 coordinate 120,227,651 (Table 4).

336 Later, we identified an additional line (BC<sub>1</sub>F<sub>4</sub> H2-18 #28-4) with a closer recombination event to  
337 *FT-A2* in the proximal region between *FT-A2-R1* and *3A-125.4*, which we planted a separate  
338 field experiment at Tulelake in the spring of 2020. This experiment included homozygous sister  
339 lines #28-4-1 and #28-4-3 fixed for either the Kronos or Gredho alleles in the segregating  
340 proximal region (Table 5), and as controls sister lines derived from plant #17-2 (Table 4) that  
341 were either homozygous for the *FT-A2* D10 (#17-2-18) or A10 allele (#17-2-22, Table 5). These  
342 two lines showed highly significant differences in SNS ( $P < 0.0001$ , Table 5) confirming that it  
343 was possible to detect differences between the two *FT-A2* alleles in this experiment. By contrast,  
344 there was no significant difference between the H2-18 #28-4 recombinant sister lines, confirming  
345 that the candidate gene was still linked to *FT-A2* (Table 5). Based on this result, we established a  
346 closer proximal flanking marker (*3A-125.4*), and reduced the candidate region for the 3AS QTL  
347 to a 5.2 Mb interval between coordinates 120,227,651 and 125,402,254 (Table 5).

348 **Genes in the candidate gene region for the 3AS QTL for SNS**

349 The annotated Chinese Spring reference genome region (RefSeq v1.1) between the two flanking  
350 markers defined in the previous section encompasses 28 high-confidence genes (including  
351 flanking genes *TraesCS3A02G141000* and *TraesCS3A02G143700*). The exome capture data  
352 revealed non-synonymous SNPs between Kronos and Gredho in only three out of the 28 genes,  
353 including the D10A polymorphism in *FT-A2*. The other two genes are described briefly below.

354 *TraesCS3A02G142200* encodes a leucine-rich repeat receptor-like protein kinase, so it is difficult  
355 to predict its potential effects. The predicted R872H amino acid change in Kronos (RefSeq v1.1  
356 3AS 121,646,195) is in a conserved region close to the end of the protein (893 amino acids) and  
357 has a BLOSUM62 score of 0, predictive of a low probability of changes in protein structure or  
358 function. The R872H polymorphism was not detected in the parental lines LA95135 and SS-  
359 MVP57 of the hexaploid winter wheat populations segregating for the 3AS SNS QTL.

360 *TraesCS3A02G143600* encodes a short peptide (104 amino acids) with a polymorphism in  
361 Kronos that generates a premature stop codon (S59\*, RefSeq v1.1 3AS 125,094,949 C to A).  
362 However, the predicted protein in Gredho also seems to be truncated since it is much shorter  
363 (104 amino acids) than the orthologous protein in wild emmer (XP\_037404892.1, 483 amino  
364 acids) or *T. urartu* (EMS53367.1, 348 amino acids). In addition, the 104 amino acids in Gredho  
365 showed no similarity to other plant proteins in the GenBank nr database in species outside the  
366 genus *Triticum*, suggesting that *TraesCS3A02G143600* encodes a non-functional protein in both  
367 Kronos and Gredho. Similar to R872H, the S59\* polymorphism was not detected in winter lines  
368 LA95135 and SS-MVP57.

369 The QTLs in the KxG and LA95135 x SS-MVP57 are co-located and affect the same traits, so  
370 we hypothesized that they should have mutations in the same gene. Therefore, we prioritized  
371 genes carrying mutations in both populations. The predicted R872H amino acid change in  
372 *TraesCS3A02G142200* was polymorphic in the KxG population but not in the winter wheat  
373 population, and the same was true for the S59\* premature stop codon in  
374 *TraesCS3A02G143600*. By contrast, the D10A polymorphisms in *FT-A2*  
375 (*TraesCS3A02G143100*) was detected in both mapping populations.

376 The R872H and S59\* polymorphisms were found in tetraploid wheat but were not detected in  
377 any of the sequenced hexaploid wheats in the wheat PanGenome project (Walkowiak et  
378 al. 2020). By contrast, *FT-A2* was polymorphic in the same group of varieties, with CDC  
379 Landmark, Lancer, and Spelt carrying the D10 allele and CS, Julius, Jagger, CDC Stanley,  
380 ArinaLRFor, Mace, Norin 61, and SY Mattis carrying the *FT-A2* A10 allele. The previous  
381 observations, together with the known effect of *FT2* mutations on SNS (Shaw et al. 2019),  
382 suggest that *FT-A2* is the most likely candidate gene in this region. However, we cannot rule  
383 out the possibility of polymorphisms shared between the two populations in the  
384 regulatory regions of other candidate genes.

### 385 **Effect of the D10A polymorphism on FT-A2 interactions with 14-3-3 proteins**

386 Previous results have shown positive interactions between FT1 and six of the seven 14-3-3  
387 proteins tested whereas FT-A2 did not interact with any of the 14-3-3 proteins (Li et al. 2015).  
388 This was a puzzling result because all other four FT-like genes showed positive interactions with  
389 at least one 14-3-3 protein. Since the original study was done using only the FT-A2 D10 allele,  
390 we decided to explore the effect of the A10 allele. In this study, both the FT-A2-D10 and FT-A2-  
391 A10 proteins failed to interact with any of the six tested 14-3-3 proteins, whereas the FT1  
392 positive control showed a strong interaction signal (Fig. S2). No autoactivation was observed in  
393 the negative controls. Given the lack of interactions between both FT-A2 alleles and any of the  
394 tested 14-3-3 protein, we have initiated Y2H screens to test if there are other protein partners of  
395 FT-A2.

396

## 397 **Discussion**

### 398 **Candidate gene and causal polymorphism**

399 In this study, we focused on SNS for the high-density mapping because this trait has a higher  
400 heritability ( $h > 0.8$ ) than other yield components (Kuzay et al. 2019; Zhang et al. 2018). Spikelet  
401 number per spike is determined early after the transition from the vegetative to the reproductive  
402 phase, when the spike meristem transitions into a terminal spikelet (Li et al. 2019). This limits  
403 the influence of later environmental variability on SNS relative to GNS or grain weight, which

404 are affected by fertility, grain abortions, and conditions affecting grain filling until the end of the  
405 season.

406 The high heritability of SNS helped us to Mendelize the QTL (using large progeny tests) and to  
407 generate a high-density map of the SNS QTL on chromosome arm 3AS. We established a 5.2  
408 Mb candidate gene region on chromosome arm 3AS including 28 annotated high-confidence  
409 genes in CS, including three with non-synonymous polymorphisms between Kronos (D10) and  
410 Gredho (A10): *TraesCS3A02G143100* (D10A), *TraesCS3A02G142200* (R872H), and  
411 *TraesCS3A02G143600* (S59\*). The last two polymorphism were detected in the Kronos x  
412 Gredho population but not in the LA95135 (D10) and SS-MVP57 (A10) suggesting that they are  
413 unlikely candidate genes for the SNS QTL, In additions, the S59\* and R872H polymorphisms  
414 were not detected among the varieties sequenced in the wheat pangenome (Walkowiak et al.  
415 2020), which suggests that they originated in durum wheat, and that the A10 mutation occurred  
416 in a haplotype different from the one present in modern durum wheat varieties (S59\*-R872H  
417 haplotype).

418 After the elimination of these two genes, *FT-A2* is the only gene in the candidate region that has  
419 a non-synonymous polymorphism (D10A) linked to the differences in SNS in both mapping  
420 populations. Although we cannot rule out the possibility of polymorphisms in regulatory regions  
421 of other candidate genes affecting SNS in both populations, the genetic data presented here,  
422 together with known effect of the loss-of-function mutations in *FT-A2* on SNS (Shaw et al.  
423 2019), point to *FT-A2* as the most likely candidate gene for the SNS QTL.

424 The D10A amino acid change in FT-A2 has a BLOSUM 62 score of -2 and is located in a  
425 conserved region of the protein, suggesting a high probability of an effect on either protein  
426 structure or function. To test if any other polymorphisms in *FT-A2* were associated with the  
427 D10A polymorphism, we compared the available exons, introns, 5' upstream region (5,000 bp)  
428 and 3' downstream region (2,000 bp) of *FT-A2* in genomic sequences of hexaploid wheat  
429 (Walkowiak et al. 2020). We did not find any additional SNPs to differentiate the varieties with  
430 the D10 allele (CDC Landmark, Lancer and Spelta) from those carrying the A10 allele (CS,  
431 Julius, Jagger, CDC Stanley, ArinaLRFor, Mace, Norin 61, and SY Mattis) in the analyzed  
432 regions. Although we cannot completely rule out the possibility of polymorphisms located in  
433 regulatory regions outside the investigated region, the available evidence points to D10A as the



434 most likely causal polymorphism. A conclusive test of this hypothesis will require the editing of  
435 the A124,172,909C, but this is not simple because this is a transversion, and currently available  
436 plant gene editors are not efficient to edit transversions. New prime editing technologies  
437 (Anzalone et al. 2019) may solve this problem once they become more efficient in plants (Lin et  
438 al. 2020).

#### 439 **Differential recombination rates within the candidate gene region**

440 The distribution of recombination events (RE) in the 10 Mb region between the flanking markers  
441 used in this study was not uniform. In the 2.4 Mb distal to the candidate gene region (117.8 to  
442 120.2 Mb, 14 genes), we detected 56 RE resulting in an average of 23.3 RE/Mb or 4.0 RE/gene.  
443 In the 2.4 Mb proximal to the candidate region (125.4 to 127.8 Mb, 13 genes), we detected 20  
444 RE resulting in a frequency of 8.3 RE /Mb or 1.5 RE/gene. Surprisingly, not a single RE was  
445 detected in the 5.2 Mb central candidate region (120.2 to 125.4 Mb, 28 genes), despite being  
446 twice as large and including twice the number of genes as the flanking regions. Recombination  
447 events occur mainly in gene regions (Darrier et al. 2017), so we would have expected to find 39  
448 of the 76 RE within the candidate region if RE were distributed proportionally to the number of  
449 genes. The same number would be expected if RE were distributed proportionally to the physical  
450 length of the interval.

451 To explore if this lack of recombination in the central region was caused by a structural  
452 rearrangement, we used the sequenced genome of the tetraploid variety Svevo (Maccaferri et al.  
453 2019) that showed the same SNPs as the Kronos exome capture across the candidate gene region.  
454 Since Gredho showed very few polymorphisms with CS across the candidate gene region, we  
455 compared the genomes of CS (A10) and Svevo (D10) in this region. In Svevo, we found  
456 orthologs to the 28 high confidence genes present in CS, with the exception of  
457 *TraesCS3A02G142500* that was present in the correct position and strand in Svevo (100%  
458 identical over all its length) but was not annotated. All the genes were in the same orientation in  
459 CS and Svevo, and the total length of the region was similar in both species (5.2 Mb), suggesting  
460 that no major structural rearrangements occurred in the candidate gene region.

461 Finally, we did a BLAST comparison of all the Svevo genes to a Kronos scaffold assembly from  
462 the Earlham Institute, U.K. and were able to detect 27 of the 28 genes with 100% identity. The

463 only exception was *TRITD3Av1G056250* (ortholog of CS *TraesCS3A02G142600*), for which we  
464 only detected the B-genome homeolog in Kronos. These results suggest the Kronos genome is  
465 not very different from Svevo in this region. We currently do not know the cause of the reduced  
466 recombination frequency between 121.5 and 125.1 Mb in the KxG population, but since no  
467 pseudomolecule assembly of Kronos or Gredho are available, we cannot rule out the possibility  
468 of structural rearrangements in this region in one of these two varieties.

#### 469 **Effect of *FT-A2* D10A polymorphism on heading time and fertility**

470 Wheat varieties are selected to flower within a narrow time window to maximize grain  
471 productivity. This limits the introgression of loss-of-function alleles that have beneficial effects  
472 on SNS but generate large delays in heading time, such as those in *VRN1* (Li et al. 2019) or  
473 *PPD1* (Shaw et al. 2013). By contrast, the *FT-A2* A10 allele has a positive effect on SNS and  
474 limited effect on heading time. Even when loss-of-function mutations in *ft-A2* and *ft-B2* were  
475 combined in Kronos, the delay in heading time was only 2-4 days (Shaw et al. 2019). In this  
476 study, the D10A polymorphism showed small effects on DTH in the different genetic  
477 backgrounds, ranging from a non-significant difference in the initial Kronos x Gredho population  
478 (Table 2), a marginally non-significant difference of 0.8 d ( $P = 0.053$ ) in the 2021 field  
479 experiment comparing Kronos isogenic lines, and an average difference of 1.7 d in the winter  
480 wheat population (Fig. 1A).

481 An important limitation for the utilization of the *ft-A2* loss-of-function mutation for wheat  
482 improvement was its negative effect on fertility (Shaw et al. 2019), which offset its positive  
483 effect on SNS, as confirmed in the 2021 Tulelake experiment in this study (Table 3). This  
484 motivated our initial search for *FT-A2* natural variants that separated the positive effects on SNS  
485 from the negative effects on fertility. Results presented in this study show that the positive effect  
486 of the A10 polymorphism on SNS were translated into positive effects on GNS in both the winter  
487 wheat population (Fig. 1e) and in the spring NILs (Table 3). In addition, this allele was not  
488 associated with negative effects on the number of grains per spikelet in any of the studied  
489 populations, suggesting that the A10 allele has no negative effect on fertility. These results  
490 provide a good example of the value of using natural variants selected by breeders to identify  
491 mutations that optimize specific traits with limited negative pleiotropic effects.

## 492 ***FT-A2* effects on SNS, GNS, grain weight and spike yield**

493 It was encouraging to see that the positive effect of the A10 allele on SNS and GNS was  
494 expressed in both winter (Fig. 1) and spring wheats (Table 3), and among the latter in both spring  
495 and fall planted spring wheats. However, the magnitude of the increases in SNS, GNS and spike  
496 yield associated with the A10 allele varied among experiments, suggesting that the effects of this  
497 *FT-A2* polymorphisms on these traits are modulated by the environment. We also observed  
498 variable effects of the A10 polymorphisms on grain weight. Whereas no significant effects were  
499 detected for this trait in the experiments performed at UCD in 2020 and at Tulelake in 2020 and  
500 2021, we detected a significant reduction in grain weight in the field experiment performed at  
501 UCD in 2021, which offset the gains in GNS (Table 3).

502 Similar observations have been reported for *WAP0-A1*, the causal gene of a wheat SNS QTL on  
503 the long arm of chromosome 7AL (Kuzay et al. 2019). Increases in SNS associated with the  
504 favorable *Wapo-A1b* allele were translated into significant increases in grain yield only when the  
505 favorable *WAP0-A1* allele was present in high-yielding / high-biomass genetic backgrounds and  
506 the plants were grown in a favorable environment. When the *Wapo-A1b* allele was present in  
507 poorly adapted varieties or when the lines were grown under water-limiting conditions, the plants  
508 did not have enough resources to fill the extra grains, resulting in a negative correlation between  
509 grain number and grain weight that limited the gains in grain yield (Kuzay et al. 2019). A study  
510 with elite CIMYT lines also highlighted the importance of genetic-by-environment interactions  
511 on the trade-offs between grain number and grain weight (Quintero et al. 2018). We hypothesize  
512 that environmental differences between our 2020 and 2021 field trials may have contributed to  
513 the observed differences in grain weight, in spite of the positive effects of the A10 allele on SNS  
514 and GNS detected in both years (Table 3). We also hypothesize that the introgression of the *FT-*  
515 *A2* A10 allele into more productive durum wheat varieties than Kronos may result in significant  
516 increases in total grain yield.

## 517 ***FT-A2* as a candidate gene for previously published SNS QTLs on chromosome arm 3AS**

518 A QTL for DTH (*Qncb.HD-3A*) was previously mapped on chromosome 3A within a 400 Mb  
519 interval including *FT-A2* (DeWitt et al. 2021) in the LA95135 x SS-MVP47 population. We  
520 found in this study that LA95135 carries the D10 allele and SS-MVP47 the A10 allele, and after  
521 genotyping the population with the *FT-A2* marker, we found that the A10 allele was associated

522 not only with a slight delay in heading time but also with higher SNS, GN, and grain yield per  
523 spike (Fig. 1). The similar pleiotropic effects of the SNS QTL in the winter wheat population and  
524 the KxG population, together with the overlapping mapping regions, suggest that the *FT-A2*  
525 D10A polymorphism may have contributed to the *Qncb.HD-3A* identified in the LA95135 x SS-  
526 MVP47 population.

527 An additional QTL for DTH was identified in the Avalon x Cadenza population (U.K.) on  
528 chromosome arm 3AS around the peak marker BS00021976 (169 Mb RefSeq v1.0) (Martinez et  
529 al. 2021). This QTL interval (60 Mb at each side of BS00021976) includes 536 annotated genes,  
530 among which the authors proposed *FT-A2* as a candidate of particular interest. Using our *FT-A2*  
531 marker, we established that both Avalon and Cadenza carry the A10 allele, so we conclude that  
532 the D10A polymorphism is not the cause for the observed QTL for DTH on 3AS in this  
533 population. Martinez et al. (2021) suggested that differences in *FT-A2* transcript levels may  
534 contribute to the differences in DTH, but more precise mapping of this QTL will be necessary to  
535 support this hypothesis.

536 Several QTLs for grain yield components have been reported in different regions of chromosome  
537 3AS in a recombinant inbred chromosome line from the cross between cultivar Cheyenne and a  
538 substitution of chromosome 3A of Wichita in Cheyenne (CNN(Wichita-3A)) (Ali et al. 2011;  
539 Campbell et al. 2003; Dilbirligi et al. 2006). QTLs for grain yield and grain number per square  
540 meter were mapped in a region between markers *barc86* and *barc67* (54.4 to 464.3 Mb RefSeq  
541 v1.0, “Region 2”) which encompasses the *FT-A2* locus. However, both Cheyenne and  
542 CNN(Wichita-3A) have the A10 allele of *FT-A2* (Supplementary Appendix S1), suggesting that  
543 a different gene (or a different polymorphism in *FT-A2*) was the cause of this QTL.

#### 544 ***FT-A2* allele frequencies and breeding applications**

545 The *FT-A2* alleles show contrasting frequencies in durum and common wheat, with the A10  
546 allele present in less than 1% of the durum accessions and in 56% of the common wheat varieties  
547 analyzed in this study (Table 1). We currently do not know if the A10 allele originated in the few  
548 durum accessions carrying this allele in Oman and Turkey, or if these represent later  
549 introgressions from hexaploid to tetraploid wheat. Independently of its origin, the frequency of  
550 the A10 allele increased rapidly since its introgression or origin in common wheat, suggesting  
551 that this allele was favored by common wheat breeders.

552 The low frequency of the A10 allele in durum wheat could be a result of infrequent gene flow  
553 from hexaploid wheat to tetraploid wheat. However, it can also be the result of selection for  
554 larger grains and indirect selection for reduced GNS in environments showing a negative  
555 correlation between these two traits. Similar to *FT-A2*, the *Wapo-A1a* allele for low SNS is  
556 almost fixed in durum wheat, whereas the *Wapo-A1b* allele for high-SNS is found at high  
557 frequencies in hexaploid wheat (Kuzay et al. 2019). We interpret this similar asymmetric  
558 distribution of *WAPO-A1* and *FT-A2* alleles for SNS in common and durum wheat as indirect  
559 support for the hypothesis that selection for larger grains may have resulted in indirect selection  
560 for reduced SNS in durum wheat.

561 Among hexaploid spring wheats, we also observed significant differences in the distribution of  
562 the *FT-A2* alleles, with a larger frequency of the A10 allele among spring varieties developed  
563 under a long growing cycle (DuF, 58.4%) than among those developed under a short growing  
564 cycle (DuS, 34.4%). We speculate that longer cycles may provide more resources to fill the extra  
565 grains associated with the A10 allele, facilitating the translation of the difference in SNS into  
566 differences in grain yield. This in turn, may result in a positive selection pressure for the A10  
567 allele in the fall-planted programs. This idea is indirectly supported by the high frequency of the  
568 A10 allele among the US winter wheat varieties (Table 1, 81.7%). Additional experiments with  
569 D10 and A10 NILs in different genetic backgrounds tested in different spring-planted and fall-  
570 planted locations will be necessary to test this hypothesis.

571 The high frequency of the A10 allele in the winter wheats and fall-planted spring wheats  
572 provides additional evidence that this allele has positive effects in those regions. However, as the  
573 frequency of the A10 allele increases, the number of varieties that can benefit from its  
574 introgression decreases. By contrast, the A10 allele is almost absent from modern durum wheat  
575 breeding programs, providing an opportunity to benefit a large proportion of these varieties. To  
576 facilitate the testing and introgression of the A10 allele into durum wheat breeding programs, we  
577 deposited the Kronos NIL with the A10 allele in the NSGC (PI 699107). Kronos is a modern  
578 durum wheat variety with excellent pasta quality, which makes it a better donor parent than  
579 Gredho.

580 Our preliminary results suggest that the A10 allele may be more beneficial in fall planted than in  
581 the spring planted durum wheat programs, but additional experiments are necessary to test this

582 hypothesis. It will be also interesting to investigate the combined effect of the A10 allele with  
583 alleles from other genes that also result in increases in SNS such as *Wapo-A1b* (Kuzay et al.  
584 2019) and the *Elf3* allele from *T. monococcum* (Alvarez et al. 2016).

585 In summary, the genetic information provided in this study, together with the previous mutant  
586 information, provides strong evidence that *FT-A2* is the causal gene for the differences in SNS,  
587 GNS, and spike yield associated with this region on chromosome arm 3AS. The identification of  
588 the likely causal polymorphism (D10A) and the development of a perfect marker for this  
589 polymorphism can accelerate the deployment of this favorable allele in wheat breeding programs  
590 worldwide.

591

## 592 **Declarations**

## 593 **Funding**

594 This project was supported by the Agriculture and Food Research Initiative Competitive Grants  
595 2017-67007-25939 (WheatCAP) from the USDA National Institute of Food and Agriculture and  
596 by the Howard Hughes Medical Institute. Priscilla Glenn acknowledges support from NSF  
597 Graduate Research Program Fellowship Grant 2036201.

598

## 599 **Acknowledgements**

600 We thank Josh Hegarty for his help with the field experiments and Youngjun Mo for the  
601 development of Kronos x Gredho population. We also thank Xiaoqin Zhang for her help with the  
602 introgression of the *A10* allele into Kronos and Saarah Kuzay for the phenotypic and genotypic  
603 data for the Kronos x Gredho population. We thank Mohammed Guedira for help with  
604 development and field evaluation of the LA95135 X SS-MPV57 population and Alina  
605 Akhunova, Mary Guttieri and Brian Ward for early access to the genotypic data for the winter  
606 wheat varieties.

607

## 608 **Conflicts of interest/Competing interests**

609 The authors declare no conflict of interests or competing interests

610

## 611 **Author contribution statement**

612 PG conducted most of the experimental work and wrote the first version of the manuscript. JZ  
613 contributed experimental work and many of the statistical analysis. KL contributed the Y2H  
614 experiments. GBG and ND contributed the LA95135 x SS-MVP57 population and the  
615 corresponding genotypic and phenotypic data. JC contributed the frequency of the D10A  
616 polymorphism in Montana spring wheat breeding lines and EA in US winter wheat lines. JD  
617 initiated and coordinated the project, contributed to data analyses, and supervised PG. All  
618 authors reviewed the manuscript and provided suggestions.

619

#### 620 **Availability of data and materials**

621 All data and materials described in this paper are available from the corresponding author upon  
622 request. The *FT-A2* introgression in Kronos is being deposited in the National Small Grains  
623 Collection (PI 699107). PI accession numbers are provided for all germplasm used when  
624 available. The datasets retrieved and analyzed during the current study are available in the  
625 T3/Wheat exome capture database (<https://wheat.triticeaetoolbox.org/>).

626

#### 627 **Code availability**

628 Not applicable.

629 **References**

- 630 Ali ML, Baenziger PS, Al Ajlouni Z, Campbell BT, Gill KS, Eskridge KM, Mujeeb-Kazi A,  
631 Dweikat I (2011) Mapping QTL for agronomic traits on wheat chromosome 3A and a  
632 comparison of recombinant inbred chromosome line populations. *Crop Sci* 51:553-566
- 633 Alvarez MA, Tranquilli G, Lewis S, Kippes N, Dubcovsky J (2016) Genetic and physical  
634 mapping of the earliness *per se* locus *Eps-A<sup>m</sup>1* in *Triticum monococcum* identifies *EARLY*  
635 *FLOWERING 3 (ELF3)* as a candidate gene. *Funct Integr Genomic* 16:365-382
- 636 Anzalone AV, Randolph PB, Davis JR, Sousa AA, Koblan LW, Levy JM, Chen PJ, Wilson C,  
637 Newby GA, Raguram A, Liu DR (2019) Search-and-replace genome editing without  
638 double-strand breaks or donor DNA. *Nature* 576:149-157
- 639 Brassac J, Muqaddasi QH, Plieske J, Ganai MW, Röder MS (2021) Linkage mapping identifies a  
640 non-synonymous mutation in *FLOWERING LOCUS T (FT-B1)* increasing spikelet  
641 number per spike. *Sci Rep-Uk* 11:1585
- 642 Campbell BT, Baenziger PS, Gill KS, Eskridge KM, Budak H, Erayman M, Dweikat I, Yen Y  
643 (2003) Identification of QTLs and environmental interactions associated with agronomic  
644 traits on chromosome 3A of wheat. *Crop Sci* 43:1493-1505
- 645 Cantu D, Yang B, Ruan R, Li K, Menzo V, Fu D, Chern M, Ronald PC, Dubcovsky J (2013)  
646 Comparative analysis of the defense response interactomes of rice and wheat. *BMC*  
647 *Genomics* 14:166
- 648 Darrier B, Rimbart H, Balfourier F, Pingault L, Josselin AA, Servin B, Navarro J, Choulet F,  
649 Paux E, Sourdille P (2017) High-resolution mapping of crossover events in the hexaploid  
650 wheat genome suggests a universal recombination mechanism. *Genetics* 206:1373-1388
- 651 DeWitt N, Guedira M, Lauer E, Murphy JP, Marshall D, Mergoum M, Johnson J, Holland JB,  
652 Brown-Guedira G (2021) Characterizing the oligogenic architecture of plant growth  
653 phenotypes informs genomic selection approaches in a common wheat population. .  
654 *BMC Genomics* 22:402
- 655 Dilbirligi M, Erayman M, Campbell BT, Randhawa HS, Baenziger PS, Dweikat I, Gill KS  
656 (2006) High-density mapping and comparative analysis of agronomically important traits  
657 on wheat chromosome 3A. *Genomics* 88:74-87



658 Finnegan EJ, Ford B, Wallace X, Pettolino F, Griffin PT, Schmitz RJ, Zhang P, Barrero JM,  
659 Hayden MJ, Boden SA, Cavanagh CA, Swain SM, Trevaskis B (2018) Zebularine  
660 treatment is associated with deletion of FT-B1 leading to an increase in spikelet number  
661 in bread wheat. *Plant Cell Environ* 41:1346-1360

662 Fox J, Weisberg S (2019) An {R} companion to applied regression (3rd edition). Sage,  
663 Thousand Oaks, California, <https://socialsciences.mcmaster.ca/jfox/Books/Companion/>

664 Gauley A, Boden SA (2021) Stepwise increases in *FT1* expression regulate seasonal progression  
665 of flowering in wheat (*Triticum aestivum*). *New Phytol* 229:1163-1176

666 Guedira M, Brown-Guedira G, Van Sanford D, Sneller C, Souza E, Marshall D (2010)  
667 Distribution of *Rht* genes in modern and historic winter wheat cultivars from the Eastern  
668 and Central USA. *Crop Sci* 50:1811-1822

669 Halliwell J, Borrill P, Gordon A, Kowalczyk R, Pagano ML, Saccomanno B, Bentley AR, Uauy  
670 C, Cockram J (2016) Systematic investigation of *FLOWERING LOCUS T*-like Poaceae  
671 gene families identifies the short-day expressed flowering pathway gene, *TaFT3* in wheat  
672 (*Triticum aestivum* L.). *Front Plant Sci* 7

673 He F, et al. (2019) Exome sequencing highlights the role of wild-relative introgression in shaping  
674 the adaptive landscape of the wheat genome. *Nat Genet* 51:896-904

675 Isham K, Wang R, Zhao W, Wheeler J, Klassen N, Akhunov E, Chen J (2021) QTL mapping for  
676 grain yield and three yield components in a population derived from two high-yielding  
677 spring wheat cultivars. *Theor Appl Genet* 134: 2079-2095.

678 Krasileva KV, et al. (2017) Uncovering hidden variation in polyploid wheat. *Proc Natl Acad Sci*  
679 U S A 114:E913-E921

680 Kuzay S, et al. (2019) Identification of a candidate gene for a QTL for spikelet number per spike  
681 on wheat chromosome arm 7AL by high-resolution genetic mapping. *Theor Appl Genet*  
682 132:2689–2705

683 Li C, Lin H, Chen A, Lau M, Jernstedt J, Dubcovsky J (2019) Wheat *VRN1*, *FUL2* and *FUL3*  
684 play critical and redundant roles in spikelet development and spike determinacy.  
685 *Development* 146:dev175398

686 Li C, Lin H, Dubcovsky J (2015) Factorial combinations of protein interactions generate a  
687 multiplicity of florigen activation complexes in wheat and barley. *Plant J* 84:70-82

688 Lin QP, Zong Y, Xue CX, Wang SX, Jin S, Zhu ZX, Wang YP, Anzalone AV, Raguram A,  
689 Doman JL, Liu DVR, Gao CX (2020) Prime genome editing in rice and wheat. *Nat*  
690 *Biotechnol* 38:582-585

691 Lv B, Nitcher R, Han X, Wang S, Ni F, Li K, Pearce S, Wu J, Dubcovsky J, Fu D (2014)  
692 Characterization of *FLOWERING LOCUS T1 (FT1)* gene in *Brachypodium* and wheat.  
693 *PLoS One* 9: e94171

694 Maccaferri M, et al. (2019) Durum wheat genome highlights past domestication signatures and  
695 future improvement targets. *Nat Genet* 51:885-895

696 Martinez AF, Lister C, Freeman S, Ma J, Berry S, Wingen L, Griffiths S (2021) Resolving a  
697 QTL complex for height, heading, and grain yield on chromosome 3A in bread wheat. *J*  
698 *Exp Bot* 72:2965-2978

699 Pearce S, Vanzetti LS, Dubcovsky J (2013) Exogenous gibberellins induce wheat spike  
700 development under short days only in the presence of *VERNALIZATION1*. *Plant Physiol*  
701 163:1433-1445

702 Poursarebani N, et al. (2015) The genetic basis of composite spike form in barley and 'Miracle-  
703 Wheat'. *Genetics* 201:155-165

704 Quintero A, Molero G, Reynolds MP, Calderini DF (2018) Trade-off between grain weight and  
705 grain number in wheat depends on GxE interaction: A case study of an elite CIMMYT  
706 panel (CIMCOG). *Eur J Agron* 92:17-29

707 Sakuma S, et al. (2019) Unleashing floret fertility in wheat through the mutation of a homeobox  
708 gene. *Proc Natl Acad Sci USA* 116:5182-5187

709 Shaw LM, Lyu B, Turner R, Li C, Chen F, Han X, Fu D, Dubcovsky J (2019) *FLOWERING*  
710 *LOCUS T2* regulates spike development and fertility in temperate cereals. *J Exp Bot*  
711 70:193–204

712 Shaw LM, Turner AS, Herry L, Griffiths S, Laurie DA (2013) Mutant alleles of *Photoperiod-1*  
713 in wheat (*Triticum aestivum* L.) that confer a late flowering phenotype in long days.  
714 PLoS One 8:e79459

715 Simmonds J, Scott P, Brinton J, Mestre TC, Bush M, Del Blanco A, Dubcovsky J, Uauy C  
716 (2016) A splice acceptor site mutation in *TaGW2-A1* increases thousand grain weight in  
717 tetraploid and hexaploid wheat through wider and longer grains. Theor Appl Genet  
718 129:1099-1112

719 Taoka K, et al. (2011) 14-3-3 proteins act as intracellular receptors for rice *Hd3a* florigen. Nature  
720 476:332-325

721 Walkowiak S, et al. (2020) Multiple wheat genomes reveal global variation in modern breeding.  
722 Nature 588:277-283

723 Wang W, Pan QL, Tian B, He F, Chen YY, Bai GH, Akhunova A, Trick HN, Akhunov E (2019)  
724 Gene editing of the wheat homologs of *TONNEAU1*-recruiting motif encoding gene  
725 affects grain shape and weight in wheat. Plant J 100:251-264

726 Wilhelm EP, Turner AS, Laurie DA (2009) Photoperiod insensitive *Ppd-A1a* mutations in  
727 tetraploid wheat (*Triticum durum* Desf.). Theor Appl Genet 118:285-294

728 Zhang JL, Gizaw SA, Bossolini E, Hegarty J, Howell T, Carter AH, Akhunov E, Dubcovsky J  
729 (2018) Identification and validation of QTL for grain yield and plant water status under  
730 contrasting water treatments in fall-sown spring wheats. Theor Appl Genet 131:1741-  
731 1759

732

733

734 **Tables**

735

736 **Table 1.** Frequency of the FT-A2 alleles in different germplasm collections

Species	Ploidy	No. acc.	A10 %	D10 %	A10	D10
<i>T. urartu</i>	2x	89	0.0%	100.0%	0	89
<i>T. turgidum</i> ssp. <i>dicoccoides</i>	4x	82	0.0%	100.0%	0	82
<i>T. turgidum</i> ssp. <i>dicoccon</i>	4x	32	0.0%	100.0%	0	32
<i>T. turgidum</i> ssp. <i>durum</i>	4x	417	0.7%	99.3%	3	414
<i>T. aestivum</i> Exome capture <sup>a</sup>	6x	238	59.7%	40.3%	142	96
<i>T. aestivum</i> US winter wheats <sup>b</sup>	6x	126	81.7%	18.3%	103	23
<i>T. aestivum</i> Spring DUF <sup>c</sup>	6x	149	58.4%	41.6%	87	62
<i>T. aestivum</i> Spring DUS <sup>d</sup>	6x	192	34.4%	65.6%	66	126

737 <sup>a</sup> He et al. 2019

738 <sup>b</sup> T3/Wheat

739 <sup>c</sup> Zhang et al. 2018

740 <sup>d</sup> Zhang et al. 2018 + 99 breeding lines from MT

741

742

743

744

745 **Table 2.** Effects of *FT-A2*, *PPD-A1* and *RHT-B1* on plant height (HT), days to heading (DTH)  
 746 and spikelet number per spike (SNS). Three-way ANOVA with *P* values of the main effects and  
 747 least-square means (LSmeans). ns = not significant, \* =  $P < 0.05$ , \*\* =  $P < 0.01$ , \*\*\* =  $P <$   
 748 0.001. All the interactions were non-significant.

		Plant height (HT, cm)	Days to heading (DTH)	Spikelet No./spike (SNS)
<i>FT-A2</i>	Kronos (D10)	113.4 ± 3.2	130.5 ± 0.9	25.1 ± 0.5
LSmean ± s.e.m.	Gredho (A10)	118.3 ± 2.2	130.6 ± 0.6	26.7 ± 0.3
Three-way ANOVA	<i>P value</i>	ns	ns	*
<i>PPD-A1</i>	Kronos	108.1 ± 2.3	120.8 ± 0.6	22.6 ± 0.4
LSmean ± s.e.m.	Gredho	121.6 ± 2.6	141.0 ± 0.7	29.6 ± 0.4
Three-way ANOVA	<i>P value</i>	***	***	***
<i>Rht-B1</i>	Kronos	97.1 ± 2.5	131.5 ± 0.7	26.2 ± 0.5
LSmean ± s.e.m.	Gredho	131.4 ± 2.8	130.2 ± 0.8	25.8 ± 0.4
Three-way ANOVA	<i>P value</i>	***	*	ns

749

750

751

752 **Table 3.** Comparisons of Near isogenic lines with the *FT-A2* A10 and D10 alleles in field  
 753 experiments at UC Davis and Tulelake in 2020 and 2021. All % changes are relative to D10.

Davis 2020	Allele	N	SNS	GN	Grains/ spikelet	GW mg	Yield / spike g	Yield / plot g
<b>Davis 2020</b>								
H2-14	D10	10 <sup>a</sup> (54 spikes)	20.27	59.22	2.92	55.81	3.31	NA
H2-14	A10	10 <sup>a</sup> (38 spikes)	21.92	70.77	3.23	56.78	4.07	NA
		A10 % change	8.1 **	19.6 ***	10.6 **	1.8 ns	22.9 **	
H2-23	D10	10 <sup>a</sup> (39 spikes)	19.36	56.31	2.91	54.47	3.07	NA
H2-23	A10	10 <sup>a</sup> (38 spikes)	23.11	81.06	3.51	54.21	4.41	NA
		A10 % change	19.4 ***	44.0 ***	20.6 ***	-0.5 ns	43.6 ***	
<b>Tulelake 2020</b>								
H2-14	D10	27 spikes	17.15	44.11	2.57	38.26	1.69	NA
H2-14	A10	23 spikes	17.83	46.48	2.61	40.49	1.88	NA
		A10 % change	4.0 ***	5.4 ns	1.4 ns	5.8 ns	11.2 ns	
<b>Davis 2021</b>								
BC <sub>4</sub> F <sub>2:4</sub>	D10	12 <sup>b</sup> (96 spikes)	18.52	67.85	3.67	60.34	4.09	1254
BC <sub>4</sub> F <sub>2:4</sub>	A10	12 <sup>b</sup> (96 spikes)	19.58	72.15	3.69	55.61	4.01	1251
		A10 % change	5.7 **	6.3 *	0.5 ns	-7.8 ***	-2.0 ns	-0.2 ns
<b>Tulelake 2021</b>								
BC <sub>4</sub> F <sub>2:4</sub>	D10	12 <sup>b</sup> (96 spikes)	15.39	41.48	2.69	58.34	2.43	746
BC <sub>4</sub> F <sub>2:4</sub>	A10	12 <sup>b</sup> (96 spikes)	16.02	44.02	2.75	59.45	2.62	854
	null	12 <sup>b</sup> (96 spikes)	16.54	40.39	2.44	54.07	2.20	789
		A10 % change	4.1 **	6.1 **	2.1 ns	1.9 ns	7.7 **	14.5 ns
		<i>ft2</i> -null % change	7.5 ***	-2.6 ns	-9.4 ***	-7.3 ***	-9.35 **	5.8 ns

754 <sup>a</sup> Experimental units were 1 m rows, with 3-5 spikes measured per row.

755 <sup>b</sup> Experimental units were 4 row plots (1.1 m<sup>2</sup>), with 8 spikes measured per plot.

756

757 **Table 4** Critical recombinant BC<sub>1</sub>F<sub>5</sub> from Davis 2019-2020 field seasons. All lines except  
 758 recombinant H2 #6 were evaluated in the 2019 field season. Comparisons of SNS for statistical  
 759 significance are only between sister lines segregating for the heterozygous region.

Marker	Chr. 3AS CS	H2	H2-6	H2-14			H2-23			D12 11-1	
		#6	#14-5	#17-2	#1-3	#18-5	#47-1	#47-5	#53-4	#71-1	#73-1
3A-117.83	117,828,272	H	H	H	H	H	K	H	H	H	K
3A-120.23	120,227,651	H	G	H	K	H	K	K	G	K	K
3A-121.48	121,482,459	H	G	H	K	G	K	K	G	K	K
3A-121.65	121,646,195	H	G	H	K	G	K	K	G	K	K
3A-122.54	122,540,617	H	G	H	K	G	K	K	G	K	K
FT-A2-L4	122,542,102	H	G	H	K	G	K	K	G	K	K
<i>FT-A2</i> SNP D10A	124,172,909	H	G	H	K	G	K	K	G	K	K
<b>SNS PHENOTYPE</b>		H	G	H	K	G	K	K	G	K	K
FT-A2-R1	125,094,949	H	G	H	K	G	K	K	G	K	K
3A-125.40	125,402,254	H	G	H	K	G	K	K	G	K	K
3A-126.57	126,567,437	K	K	H	K	G	K	K	G	K	K
3A-127.82	127,821,835	K	K	K	K	G	H	K	G	K	H
Number of plants in PT		34	83	71	72	79	70	74	75	80	81
SNS Avg. Gredho allele (G)		22.1	23.9	23.5	22.4	24.2	22.4	22.7	24.1	22.3	23.1
SNS Avg. Kronos allele (K)		21.6	23.2	21.7	22.5	23.0	21.9	22.4	24.3	21.7	22.4
P values K vs G		3e-05	NS	0.004	NS	NS	NS	NS	NS	NS	NS

760

761

762 **Table 5** Spikelet number per spike (SNS) evaluation of BC<sub>1</sub>F<sub>6</sub> homozygous sister lines from  
 763 recombinant line H2-18 #28-4 in Tulelake 2020. Sister line #28-4-#1 carried a proximal Kronos  
 764 chromosome segment and sister line #28-4-#3 a proximal Gredho chromosome segment. Lines  
 765 #17-2-18 (*FT-A2* D10) and #17-2-22 (*FT-A2* A10) were included as controls.

Marker	Chr.3AS CS	H2-18	H2-18	H2-14	H2-18
		#28-4-1	#28-4-3	#17-2-18	#17-2-22
3A-117.82	117,828,272	G	G	K	G
3A-120.2	120,227,651	G	G	K	G
3A-121.4	121,482,459	G	G	K	G
3A-121.64	121,646,195	G	G	K	G
3A-122.540	122,540,617	G	G	K	G
FT-A2-L4	122,542,102	G	G	K	G
<i>FT-A2</i> SNP D10A	124,172,909	G	G	K	G
<b>SNS PHENOYPE</b>		G	G	K	G
FT-A2-R1	125,094,949	G	G	K	G
3A-125.4	125,402,254	K	G	K	G
3A-126.5	126,567,437	K	G	K	G
3A-127.8	127,821,835	K	G	K	K
Number of plants		40	42	43	40
SNS Avg		17.68	17.87	16.94	17.94
<i>P</i> values D10 (K) vs A10 (G)		0.287		1.78E-09	

767

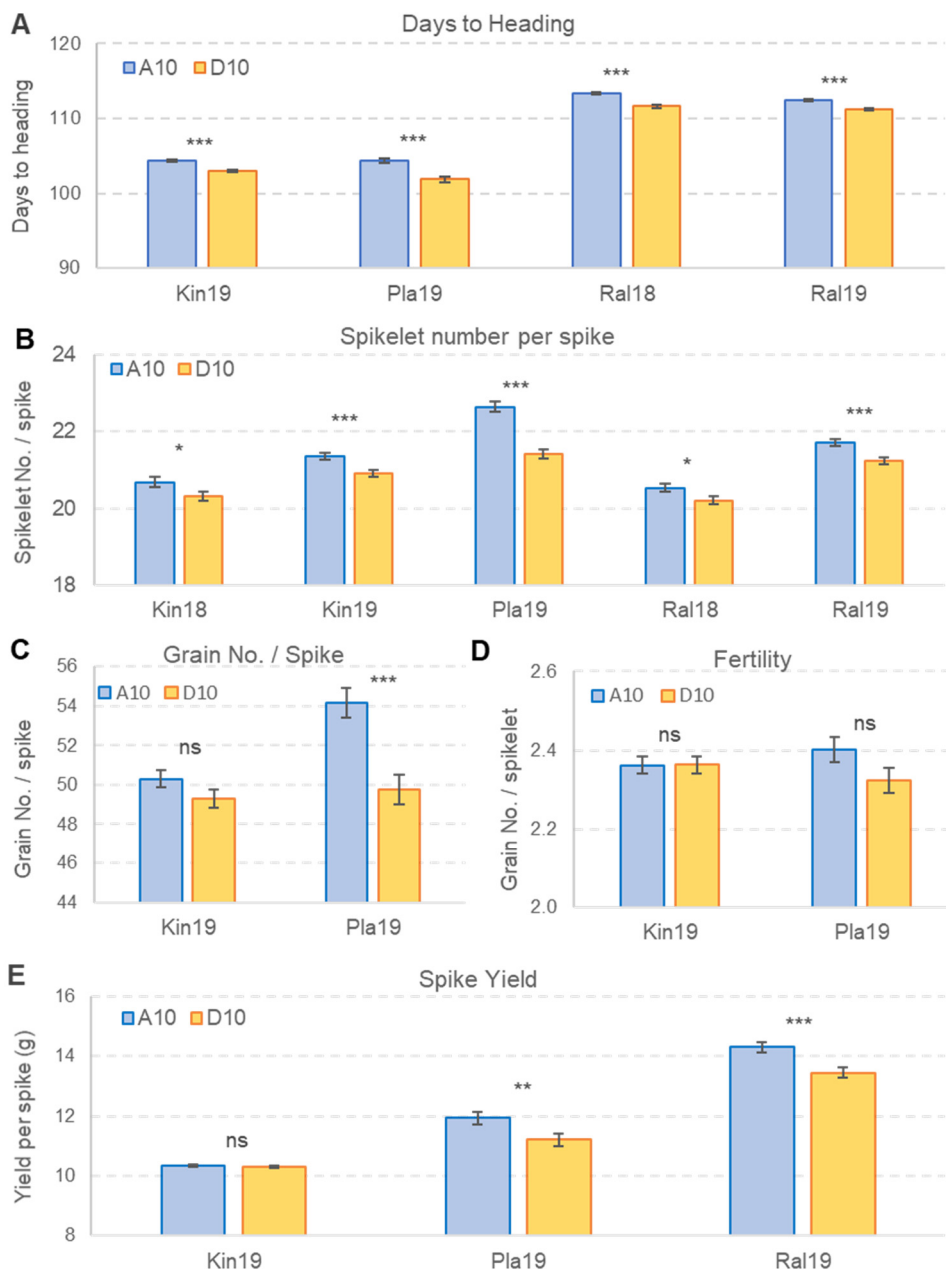
768

769



770 **Figure legends**

771 **Fig. 1** Comparison between *FT-A2* A10 (SS-MVP57) and D10 (LA95135) alleles in winter  
 772 wheat. **a** Days to heading. **b** Spikelet number per spike. **c** Grain number per spike. **d** Grain  
 773 number per spikelet (fertility). **e** Average spike yield. Bars are least square means from a  
 774 factorial ANOVA including *PPD-D1*, *RHT-D1* and *WAPO-A1* as factors. Error bars are s.e.m.  
 775 ns= not significant, \*  $P = 0.05$ , \*\*  $P = 0.01$ , \*\*\*  $P = 0.001$ .



776